Trace-Orthogonal PPM-Space Time Block Coding under Rate Constraints for Visible Light Communication*

M. Biagi, A.M. Vegni, S. Pergoloni, P. Butala, and T.D.C. Little†

December 23, 2014

MCL Technical Report No. 12-23-2014

Abstract–Visible Light Communications (VLC) represents a new frontier of communications allowing high data-rate Internet access, specially in indoor environments, where the use of Light Emitting Diodes (LEDs) is growing as a viable alternative to traditional illumination. As a result, LED output intensity can be varied faster than human eye can perceive, thus guaranteeing simultaneous wireless communications and illumination. One of the key challenges is the limited modulation bandwidth of sources that is typically around several MHz. The use of Multiple Input and Multiple Output (MIMO) techniques in optical wireless system helps to increase the capacity of the system and thus improve the system performance. In this paper we investigate the use of an optical MIMO technique jointly with Pulse Position Modulation in order to improve the data rates without reducing the reliability of the link. PPM is known to be Signal-to-Noise Ratio efficient modulation format, while it is bandwidth inefficient so the use of MIMO can compensate that drawback with reasonable complexity. Furthermore, an off-line tool for VLC system planning, including error probability and transmission rate, has been proposed in order to solve the trade-off between transmission rate and error rate. Finally, several numerical results and performance comparisons are reported.

*In *J. of Lightwave Technolgy*, January 2015. This work is supported by the NSF under grant No. EEC-0812056. Any opinions, findings, and conclusions or recommendations expressed in this material are those of the author(s) and do not necessarily reflect the views of the National Science Foundation.

†M. Biagi and S. Pergoloni are with the Department of Information, Electronics and Telecommunication Engineeering (DIET), University of Rome "Sapienza", Rome, Italy, via Eudossiana 18, 00148 Rome, Italy, {*mauro.biagi, stefano.pergoloni*}*@uniroma1.it*. A.M. Vegni is with the Department of Engineering, COMLAB Telecommunications lab, Roma TRE University, Rome, Italy, *annamaria.vegni@uniroma3.it*. T.D.C. Little and P. Butala are with the Department of Electrical and Computer Engineering, Boston University, Boston, MA USA {*tdcl, pbutala*}*@bu.edu*.

1 Introduction and goals

Recently, the scientific community has paid significant attention to Visible Light Communications (VLC) systems, since the idea of using the same light source for illumination, as well as to provide wireless connectivity, may allow a more flexible way to access the Internet, and makes simple hardware installation [1, 2].

In this "dual-use" paradigm, VLC offers several advantages that make it a great complement to the well-established Radio-Frequency (RF) communications. Among the main advantages belonging to VLC, we cite (*i*) the free use of the visible light spectrum, (*ii*) the directional nature of optical transmissions allowing coexistence of many non-interfering links in close proximity, and (*iii*) the secure indoor transmission. These features enable greater data rate densities [Mbit/s/m^2], as well as improved security, compared to traditional RF systems [3].

In contrast to optical communications in the Infrared (IR) and Ultraviolet (UV) wavelengths, VLC is safer to human eyes, because intense visible light triggers the blinking reflex, preventing prolonged exposures. Much higher transmission powers are then allowed by eye safety regulations [4]; as a result, the ubiquity and the high illumination levels required for indoor lighting bodes well for VLC to provide area coverage and link robustness at high receive powers, even in absence of Line-of-Sight (LOS) links.

Bandwidth-efficient encoding schemes, such as Pulse Amplitude Modulation (PAM) and Quadrature Amplitude Modulation (QAM), are also used to increase data rate, assuming that a higher requirement for signal power is met. These have been combined with Discrete Multi-Tone (DMT) modulation to reach data rates of more than 800 Mbit/s in the lab [5, 6].

The main drawback of bandwidth-efficient modulation schemes and multi-carrier schemes such as DMT is power inefficiency. This inefficiency is twofold. First, the QAM-like modulations loaded on sub-carriers are power inefficient, and second there is the requirement of additional energy to map the constellation in the first quadrant, and so a bias light is needed. Even if in the literature some schemes proposed an interesting modified version of DMT reducing the bias requested for enabling transmission (see [7] and [8]), they well perform under the assumption of Additive White Gaussian Noise (AWGN) environment without taking care of path-loss (that in general reduces the distance among symbols) and, more, these contributions do not solve the lack of power efficiency typical of QAM modulations operated on OFDM sub-carriers.

A way to improve system performance may be the use of diversity. This requires the knowledge of how many and which LEDs are able to serve an end-user especially in large rooms; as a consequence, information about positioning is mandatory. However, having a module for transmission/reception and one for positioning can be costly. This strongly motivates the use of *on-off* schemes, such as Non-Return-to-Zero or Pulse Position Modulation (PPM) for VLC, since it can be used both for positioning and transmission. Moreover, in this contribution we consider only downlink transmission even if, it is reasnable that in the near future also optical wireless uplink will be considered. Hence it is expected a grow of the need of power efficient modulation formats [9, 10]. Finally, PPM transmission can be helpful for localization by using the same transmitter controller (see [11]), and it is interesting to evaluate how this Signal-to-Noise Ratio (SNR)-efficient[1] modulation can be stressed in terms of transmission rate.

[1]We use the term SNR-efficient to indicate that an orthogonal modulation, as PPM, requires lower SNR for an assigned error rate when the number of symbols of PPM increases.

1.1 Related Work

In indoor environments, illumination is typically provided by arrays of "white" LEDs working as sources that can provide sufficient light to achieve an illumination of $[400–800]$ lux at the height of a table [12]. In such systems, high power levels are available for communication, leading to very high SNR channels [13] as compared to traditional IR free space communications. However, when 'white' phosohor-converted LEDs are used, the modulation bandwidth is limited to several MHz, due to the slow response time of the yellow phosphor that is used to generate part of the white light spectrum.

For implementation simplicity and cost, Optical Wireless (OW) systems for indoor use will employ single-element transmitters and receivers. However, the adoption of MIMO solutions have the potential to substantially improve capacity by the use of laser and photodiode arrays so that incoming data is parallelized and transmitted over multiple beams. OW MIMO links require spatial alignment among the transmitter and receiver arrays in order to avoid interference between the channels or techniques to subsequently resolve signal overlap at the receiver. On the other hand, in OW MIMO link, a Spatial-Light Modulator (SLM) can be implemented as a transmitter, and an array of optical intensity receivers as a single receiver, so that data is sent by creating a series of two-dimensional optical intensity images (see [14]).

MIMO techniques are largely used in radio communications [15], where scattering and interference create channels decorrelated from each another. This allows MIMO channels having higher capacity than the Single Input Single Output (SISO) scheme. The availability of a large number of high SNR channels with low bandwidth makes MIMO techniques an attractive solution for achieving high data rates, resulting in data transmissions in parallel between multiple sources and multiple receivers. In this regard, in [16] a MIMO VLC system architecture has been proposed, with the aim of maximizing capacity, while maintaining illumination requirements.

The use of MIMO together with a space-time coding technique can provide large gains in spectral efficiency. For instance, reference [17] combines Orthogonal Frequency Division Modulation (OFDM) with Spatial Modulation to provide better spectral efficiency. MIMO can highly increase the transmission capacity of a wireless optical communication system, while not excessively increasing the spectral bandwidth [18]. Moreover, through the use of *spatial diversity* it is possible to mitigate channel fading.

A recent trend emerging in VLC systems research is the use of organic devices *i.e.*, organic photodetectors (OPD), and organic LEDs (OLEDs) [19]. Organic small molecules and polymer photonic devices are the focus of wide ranging research due to fascinating characteristics such as mechanical flexibility, and very low cost solution-based processing. Moreover, the use of organic devices in VLC systems promises high luminous efficacies of 100 lm/W, which are into line with traditional white LED luminous efficacies (*i.e.*, around 120 lm/W). In [20] Haigh *et al.* present an experimental demonstration of a MIMO VLC system comprised of four silicon (Si)-LEDs and four OPDs using On-Off Keying (OOK) modulation format that can reach a data rate of 200 kb/s without the need for equalization. Then, through the use of an artificial neural network, which has been assessed as the most effective method for reducing Inter-Symbol Interference (ISI) induced by a communication channel, the bit rate increases to 1.8 Mb/s. In order to increase the data rate of a VLC system, Haigh *et al.* [21] exploit equalization techniques. They present two VLC links comprised of (*i*) a (Si)-LED, and an OPD, and (*ii*) an OLED plus a Si-PD, and implement digital FIR post-equalizers with and without distortion. For both systems, the bit rates achieved

are 750 kb/s and 550 kb/s, from a raw bandwidth of 30 kHz, and 93 kHz, respectively.

Because OW signals, unlike RF, are intensity modulated and non-negative, the signal mapping for OW must be treated differently. For shorter range systems, Jivkova *et al.* [22] proposed a novel MIMO approach to model an indoor system, and focused on the capacity of a MIMO system. The possibility of using MIMO transmission/reception schemes for OW systems has been already introduced in [23], considering a MIMO-LED scheme based on imaging with 4 LEDs and 4 photodiodes. Also in [24], a MIMO approach has been assumed by evaluating performance of different modulation schemes under the hypotheses of both alignment and unaligned alinks mong LEDs and photodiodes.

A number of indoor optical wireless studies and experiments have been undertaken [25–33]. In [25], Fath and Haas compare the performance of MIMO techniques applied to indoor optical wireless communications, under the assumption of Line-of-Sight (LOS) channel conditions. Several 4×4 setups with different transmitter spacing and receiver array positions are considered, as well are different MIMO algorithms *i.e.*, Repetition Coding (RC), Spatial Multiplexing (SMP), and Spatial Modulation (SM). The SM approach is a combined MIMO and digital modulation technique. Results have assessed that SM is more robust to high channel correlation, as compared to SMP, while enabling larger spectral efficiency as compared to RC. However, in [34], the authors show significant performance improvements over the work in [25], by using imaging receivers.

SM has recently been established as a promising transmission concept [27, 28], belonging to the single-RF large-scale MIMO wireless systems family. Indeed, SM can be regarded as a MIMO scheme that possesses a larger set of radiating elements, and takes advantage of the whole antenna-array at the transmitter, whilst using a limited number of RF chains. In this way, SM-MIMOs can provide high-rate systems. Again, Fath and Haas in [26] have addressed the performance of optical SM, while using narrow wavelength (colored) LEDs. Indeed, they proved that colored LEDs can improve the performance of SM by more than 10 dB, due to the fact that the responsivity of photodiodes is a function of the optical wavelength.

In reference [35], results from several indoor communications experiments are reported, considering a four channel MIMO system using "white" LEDs. Moreover, in [36], Park *et al.* design a spatially multiplexed optical wireless MIMO system, which supports two data streams simultaneously based on the singular value decomposition of the channel matrix and the adaptive modulation. The goal is to maximize data rate under the constraints of non-negativity, summed optical power, and the target BER. They also propose a new allocation method to find the optical power, the offset, and the modulation size for each data stream for optical wireless MIMO channels.

Experimental studies related to VLC systems have been presented in references [37–40]. In [37], Burton *et al.* provide a demonstration of an indoor non-imaging VLC MIMO system that can achieve a bit rate of 50 Mb/s over a distance of 2 m. The system has been assessed for different detection methods *i.e.*, from the basic channel inversion to space-time techniques. In [38], Wu *et al.* demonstrate a 1.1-Gb/s VLC system employing Carrier-less Amplitude and Phase modulation (CAP) that is the scheme of QAM for single carrier systems. Using CAP modulation, two orthogonal signals do not need overhead and carrier; indeed, the CAP modulation is carrier-less, and then, it is more suitable for band-limited intensity-modulated single carrier systems.

In [39], Khalid *et al.* demonstrate a VLC system comprised of a white LED and an avalanche photodiode (APD) receiver, achieving a data rate of 1 Gb/s at a standard illuminance level and with a BER of 1.5×10^{-3}. The proposed approach uses an optimized DMT modulation technique, and adaptive bit- and power-loading algorithms. Finally, in [40], Choi *et al.* provide experimental re-

sults for a low data rate VLC system, by using PPM and PWM (Pulse Width Modulation) formats, respectively for data communications and dimming. The authors demonstrate that in a typical indoor environment, independent control of light dimming is possible while transmitting data, under the assumption that the PWM dimming period is an integer multiple of the PPM slot duration.

On the use of techniques based on angle diversity on the receiver, Tsonev *et al.* [41] investigate how to enhance MIMO OW systems by exploiting such an approach. The authors illustrate a MIMO OWC system with an angle diversity receiver comprised of multiple detector elements. Such receivers are able to successfully identify transmitter directions, since at any given time, each transmitter is within the Field of View (FOV) of at least one detector. The authors investigate scenarios including 4×4, and 16×16 MIMO configurations.

The use of diversity techniques, such as Maximum Ratio Combining (MRC), can further enhance the performance of the optical wireless system, and Space-Time Block Coding (STBC) MIMO techniques have proven to be very promising [15]. As an instance, in [42] Ntogari *et al.* introduce a diffuse Alamouti-type STBC for MIMO system, and exploit DMT in order to mitigate the effect of ISI due to the channel's impulse response. The performance of STBC systems, employing two transmit elements, is compared against SISO and MRC systems. It has been proven that STBC techniques can be used to (*i*) increase the capacity of diffuse optical wireless systems, (*ii*) improve their coverage, and also (*iii*) decrease the required optical power at the transmitter.

Furthermore, in [43] a Multiple-Input Single-Output (MISO) scheme has been considered, working jointly with PPM. In this contribution, space-time coding it is not adopted, while different symbol mapping is used to guarantee reliable performance in terms of error probability. The scheme is simple to implement, even if it does not consider imperfect channel estimation available at the receiver *i.e.*, the channel is not perfectly known at the receiver.

Moreover, the works in references [44–47] deal with an approach for merging PPM and MIMO. Specifically, they propose schemes employing Ultra Wide Band radio techniques in order to translate the full diversity criterion, originally developed for non orthogonal modulations [48], for the orthogonal modulation case.

Lastly, the approaches following in references [49], [50] and [51] resort to repetition coding jointly with the use of MIMO, and also compare the performance obtained with conventional STBCs even though both [50] and [51] require the use of lasers because they are proposed for outdoor scenarios. Interestingly, these schemes perform well from a BER standpoint, but do not focus on transmission rate reduction with respect to conventional STBC schemes required to achieve the error rate gain. In other words, they aim at optimizing BER despite performance degradation in the transmission speed.

1.2 Goals

The main motivation behind this work is to give an additional element in the literature panorama for another possible candidate enabling Light-Fidelity (Li-Fi) wireless connections [52] as a form of VLC. In this paper we propose a MIMO-LED architecture with STBC based on PPM modulation, with a special focus on flexibility; the system we propose is able to meet constraints in terms of Bit Error Rate (BER), as well as transmission rate.

Several contributions in the literature, mainly related to RF links and dealing with STBCs, emphasize the ability of these codes to allow very low BERs with interesting power saving properties. In fact, the behavior of such codes is to present a relationship between SNR and BER (or Error

Probability) that is, in the best case (see [15]), $\Pr\{e\} \propto (c \cdot SNR)^{-div}$, where c is the so called coding gain, and div is the product of the transmission and receive elements (full diversity). This gain can be achieved at the expense of a transmission rate reduction, since not all the codewords combination possibilities are explored. On the other hand, SMP uses all the possible codewords combinations, so maximizing the transmission rate without (necessarily) achieve full diversity.

This paper tries to follow the so called *via media* that is the road in the middle between high transmission rate and reliability. In fact, the proposed scheme is flexible since, starting from (possible) requirements in terms of rate and error probabilities, it *offline* maps bits in the the codewords, meeting these constraints according to the (information conservative) criterion of *Trace Orthogonal* (TO in the following, see [53] where TO has been proposed for *non-orthogonal* modulations), which is able to give rise to a reliable error probability performance, evaluated via union bound based on pairwise probability. The use of PPM modulation format is driven by *i)* its sufficiently simple implementation that it is not so different from the widely used OOK, even if the performance is better and *ii)* its capability to be SNR-efficient, that is, BER decreases when the number of PPM symbols increases [54] at the expense of rate that can be compensated thanks to the use of spatial diversity. Furthermore, PPM allows the space-time matrix to have some interesting properties [11], as it will be highlighted in the next sections. Furthermore, PPM carries information on delay and this last is strongly related to position acquisition (see [11]). In fact, generally it is not assured that all the LEDs in a room can offer connection to a device and, in this sense, having information about position can help to select the LEDs for performing space-time coding. In other words, the knowledge of receiver position can be useful in those scenarios characterized by large rooms and high number of LEDs, since it is possible that only few LEDs can serve the reference user. This justifies the need for positioning so as to select those LEDs able to operate the STBC for the reference user, and PPM can aid this operation. Finally, some impairments will be considered, as the effect of imperfect channel knowledge, and propagation environment reflecting on channel delay spread and also spatial correlation.

This paper is organized as follows. The analytical model is introduced in Section 2, where we give background on existing VLC approaches for indoor wireless communications, including a description of the relevant characteristics of the channel model. In Section 3, we define the proposed MIMO-LEDs architecture based on PPM-STBC technique, and also address considerations on modeling of receiver architecture. In Section 4, numerical results are expressed in terms of BER and achievable data rates. Finally, conclusions are drawn in Sect.5.

2 Indoor Optical Wireless Communication Essentials

All optical wireless communications, including VLC, use Intensity Modulation and Direct Detection (IM/DD). We consider the following link model, in which a desired transmitted optical intensity waveform $x(t)$ of T_p [s] time duration arrives distorted at a photodiode receiver. It will produce an electrical current $y(t)$ proportional to $x(t)$, whose expression is:

$$y(t) = rA_e x(t) * h(t) + w(t), \tag{1}$$

where r [A/W] is the responsivity of the photodiode, A_e [m^2] is the effective receiver area, $h(t)$ is the convolutive channel impulse response, and $w(t)$ is whole noise due to ambient light, nominally Poisson distributed [55] and additive white Gaussian thermal noise. About the impact of different

factors, A_e depends on the actual photodiode area, the angle of light incidence, and the concentrator used [56,57]. Also, the responsivity r varies with the color spectrum of the light that is incident on the photodiode surface, which in turn depends on the spectrum of the LED source, as well as on any color filter used at the receiver.

For sufficiently low rates, *i.e.*, $\mathcal{R}$ [bit/s] of the order of few Mb/s, the channel is close to be ideal (*i.e.*, $h(t) = H_0\delta(t)$), while for higher rates, the signal distortion becomes important and not negligible, since it may cause inter-pulse (and/or inter-symbol) interference. A very good short-hand predictor of optical link performance in the presence of distortion is root mean square (r.m.s.) delay spread of the response $h(t)$. Namely, r.m.s delay spread must be short compared to the symbol time (*i.e.*, $T_s = \mathcal{R}^{-1}$), in order to avoid significant effects from ISI, [58].

Dealing with channel modeling, "white" and "blue" channel impulse responses are represented by $h_w(t)$ and $h_b(t)$, respectively. The term $h_w(t)$ includes distortions introduced by (*i*) the "white" LED *i.e.*, $g_w(t)$, (*ii*) the free-space signal propagation, including multipath *i.e.*, $g_f(t)$, and (*iii*) the receiver *i.e.*, $g_r(t)$, as follows:

$$h_w(t) = g_w(t) * g_f(t) * g_r(t). \tag{2}$$

As mentioned early, we consider "white" LEDs optimized for illumination and, as a result, the choice of design parameters is very limited. Indeed, currently available "white" LEDs are constructed from a $\approx$ 450 nm "blue" LED chip encased in a phosphor material that converts blue light to a broad spectrum yellow. The combination of the blue light that escapes unchanged, plus the yellow phosphor light, appears white to humans. Only the blue component is modulated directly, while the yellow one responds to blue pulses with a delay and a longer phosphorescence effect. This is mathematically expressed by means of the following "white" LED impulse response $g_w(t)$, as a combination of multiple terms:

$$g_w(t) = g_b(t) + g_y(t), \tag{3}$$

where $g_b(t)$ and $g_y(t)$ are respectively the blue and yellow portions of "white" LED response $g_w(t)$, corresponding to a 3-dB modulation bandwidth of about 2 MHz (see [59] and [60]). The blue portion $g_b(t)$ intrinsically may have a 3-dB bandwidth up to 20 MHz, which can be accessed by removing the yellow contribution by using a 450 nm bandpass optical filter placed in front of the receiver. This allows to represent the "blue" channel impulse response $h_b(t)$ as:

$$h_b(t) = g_b(t) * g_f(t) * g_r(t), \tag{4}$$

which implies a lower received signal power in blue range than the white, mainly due to removing g_y, which is the slower modulated signal emitted by the phosphor at longer color wavelengths [2].

In our model, we will use the approximated response for a "white" Luxeon Star LED, as measured in [59], which is quite representative of other LEDs. The fit for the blue-only channel is $G_b(\omega) = e^{-\omega/\omega_1}$, with $\omega_1 = 2\pi \times 15.5 \times 10^6$ rad/s. This approximation gives $g_b(t)$ with a r.m.s. delay spread of 10.2 ns [3]. For the "white" modulation response, it can be approximated similarly as:

$$G_w(\omega) = \begin{cases} e^{-\omega/\omega_2}, & \text{if } \omega < \omega_c \\ e^{-\omega_c/\omega_2} \cdot e^{\omega_c/\omega_3} \cdot e^{-\omega/\omega_3}, & \text{if } \omega > \omega_c \end{cases} \tag{5}$$

[2]Note that this filter also reduces shot noise by rejecting DC ambient light in the environment at those wavelengths.

[3]These values come directly from the LED and photodiode considered in the paper and, more, from the channel model.

where $\omega_2 = 2\pi \times 3.26 \times 10^6$, $\omega_3 = 2\pi \times 10.86 \times 10^6$ and $\omega_c = 2\pi \times 10^6$ rad/s. The corresponding delay spread is 47.5 ns. The free-space channel $g_f(t)$ has a relatively smaller delay spread, though it depends on whether the link is (*i*) Line-Of-Sight (LOS), or (*ii*) Non LOS (NLOS, also known as "shadowed") [54].

Leveraging these considerations, we can resort to the classification provided by Kahn and Berry [54], and consider three different cases of interest for channel modeling:

1. *Directed LOS channel* (*LOS*), with attenuation but negligible multipath component, *i.e.* $g_f(t) \approx H_0\delta(t)$. This type of channel occurs with short distance LOS links (around tens of centimeters), [59];

2. *Non-Directed LOS channel* (*ND-LOS*), with LOS component but also significant delayed components due to reflected secondary paths. The energy is spread over time, resulting in a reduction of the converted current at the photodiode. This scenario matches well with a transmission at $[1–2]$ meters so the diversity gain is expected to be higher than that of *LOS*;

3. *NLOS channel or diffuse* (*NLOS*), with no LOS paths due to shadowing. The link relies on collecting only the reflected paths, leading to inter-symbol and inter-pulse interference. Moreover, pulse overlapping can occur if the PPM transmission rate is higher with respect to (w.r.t.) the reciprocal of channel delay spread. The diversity gain is then expected to be high, and in the case of very high PPM rate for single LED scenario, equalization is required. However, in the proposed MIMO-PPM approach, no equalization is expected since our technique can increase rate without stressing the time domain.

Notice that a receiver can be chosen to greatly outperform the LED and the channel in terms of bandwidth. For example, Minh *et al.* in [59] use a 15 mm^2 active area PIN receiver with a 77 MHz bandwidth. Therefore, we can assume $g_r(t) = \delta(t)$. This assumption is in line with the simultaneous use of *blue* component and simple post-equalization techniques like that proposed in [59].

A typical behavior for the channel impulse responses is depicted in Figure 1 for the cases *LOS*, *ND-LOS*, and *NLOS*. We notice that *LOS* presents higher gain, and exhibits lower delay –for the first path–, while *ND-LOS* and *NLOS* present lower gain (*i.e.*, higher attenuation), while having higher delays. This plot has been obtained by posing the reference receiver in different places in the room –corresponding to a grid mapping the entire $6m \times 6m$ room with distances of 0.25 meters–, and we also averaged the received signal power by dividing the propagation environment in the above three different zones (*i.e.*, *LOS*, *ND-LOS*, and *NLOS*). These results are obtained by channel modeling simulations using CandLES (see [61] for exhaustive details). The simulation considers reflections in a ray-tracing like fashion including the presence of obstacles such as walls and furniture.

The details about LEDs and photodiodes, as well as reflectivities and other parameters, are reported in Table 1. The CandLES software simulation provides the multipath impulse response at each receiver. The channel model used by CandLES is able to combine signals from multiple transmitters as measured at multiple receivers. This functionality is currently used for volumetric analysis of communications performance, and modeling of synchronized or array-based LED transmitters. As an example, situating multiple autonomous transmitters into the environment will allow CandLES to quantify the interference among them.

Table 1: Model Parameters

LED Transmitter	
Maximum transmit sum power (white) P_t	1 W
Beam angle	45° FWHM (Full Width Half Maximum)
Room setup	
Dimensions ($l \times w \times h$)	6 m $\times$6 m $\times$3.2 m
Surface reflectivities	0.8
Ambient (DC) irradiance	5.8μW/(cm$^2\times$ nm)
4 LEDs coordinates	$(2,2)$, $(2,4)$, $(4,2)$, $(4,2)$
Photodiodes spacing	20 cm
Receiver	
FOV	90°
Area	15 mm^2
Lens gain factor	2.2
Effective area A_e	33 mm^2
Optical filter	450 ± 20 nm, 60% through
Responsivity @450 nm	0.2 A/W
Responsivity @650 nm	0.4 A/W
Load resistor	750 Ohms

3 Trace-Orthogonal MIMO-PPM

Before describing the proposed approach, recall that the *features* that a good communication system must retain are high transmission rate and low error rate. It is well known that these metrics must be traded off. We focus on achieving a minimum (not low) required rate using MIMO and STBC, under a constraint on bit error probability.

We start from a model where the channel is flat w.r.t. the frequency response (*i.e.*, *LOS* scenario). We assume n_T and n_R as the number of LEDs and photodiodes at the transmitter and the receiver sides, respectively. The wireless-optical link is characterized by different LEDs placed on the ceiling of a room. The LEDs are required to be positioned such that sufficient light coverage (illumination) is provided and that the LEDs can reliably provide communication, and when defined, reduce ambiguity in indoor positioning (e.g., [62]). Moreover, the LED placement should be achieved to guarantee diversity gain, that is, spatial uncorrelation among channels. As will appear clearer in the following, the channel features strongly influence performance not only in terms of attenuation.

In our scheme, the received signal can be written in the following way

$$\mathbf{Y} = \mathbf{XH} + \mathbf{W}, \tag{6}$$

where $\mathbf{Y}$ is the $[L \times n_R]$ matrix collecting the L-PPM symbols received by the n_R photodiodes and

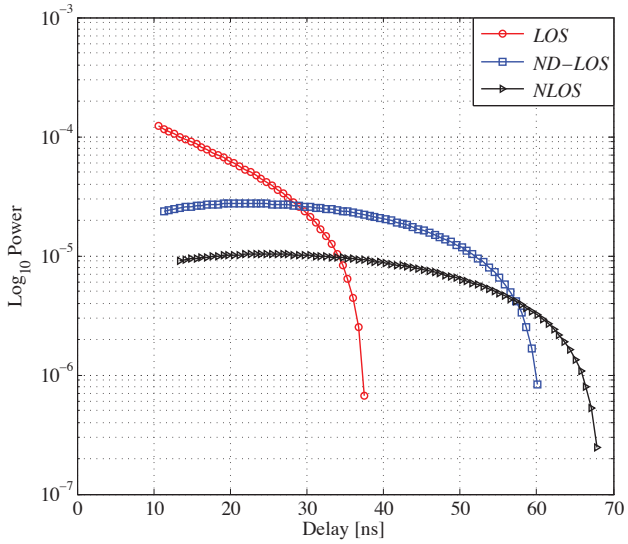

Figure 1: Log-description of power received in *LOS*, *ND-LOS*, and *NLOS* propagation environment.

H is a $[n_T \times n_R]$ matrix, where each element in the position (i, j) is the channel path between the i-th transmitting LED and the j-th receiving photodiode. The term **W** is a $[L \times n_R]$ matrix, describing thermal and ambient noise. Last, **X** is the STBC $[L \times n_T]$ matrix that carries information according to the cardinality of L-PPM and the number of transmitting LEDs. As previously anticipated, PPM is chosen for its easy implementation, since the circuit generating pulses is the same as for On-Off Keying. It is well known from the literature that PPM is a good modulation format for reducing BER, while it has poor performance in terms of rate. This effect is counterbalanced by the use of the MIMO architecture, as it will be shown later in this work.

Equation (6) is a discrete-time representation of what is present at the receiver photodiodes. Each of the n_R photodiodes receives n_T analog signals coming from the n_T transmitting LEDs and filtered by the channels. The analog baseband signal can be represented by resorting to (1), where $X(t)$ is the signal emitted by a generic LED. When multiple LEDs are available at the transmitter side, the columns of **X** are the discrete time representation of what is emitted by the LEDs. In particular, by selecting the i-th column and by spanning its elements, we can identify what the i-th LED is transmitting; whereas by observing the n-th row, it is possible to appreciate, at n-th time, what all available LEDs are emitting.

The corresponding (analog baseband) signal *i.e.*, $y_j(t)$, measured at the output of the j-th receive photodiode[4] over a signaling period $T_s = T_p + T_g$ (with T_p the pulse period, and being T_g a guard-time interval), can be expressed in its general form as

$$y_j(t) = \frac{1}{\sqrt{n_T}} \sum_{i=1}^{n_T} h_{ij}(t) * X^{(i)}(t) + W_j(t) =$$

$$= \frac{1}{\sqrt{n_T}} \sum_{i=1}^{n_T} \left[\sum_{n=0}^{V} h_n(i,j) X^{(i)}(t - \tau_n(i,j)) \right] + W_j(t),$$

[4]We assume a uniform distribution of the light on the surface of photodetector.

$$\text{with } \; 0 \leq t \leq T_s, \; 1 \leq j \leq n_R, \tag{7}$$

where $w_j(t)$ are the noise components at each receive photodiode, $h_{ij}(t)$ is the continuous time channel impulse response related to the channel from the i-th LED to the j-th photodiode, while $h_n(i,j)$ is the amplitude of one out of $(V+1)$ paths associated to the $\tau_n(i,j)$ delay of $h_{ij}(t)$. The normalization is to reconcile the need for equal power transmitters, that is, to compare links with the same power emitted. Moving from $y_j(t)$ to $\mathbf{y}_j[n]$ can be obtained by sampling the output at the pulse period T_p, as

$$\mathbf{y}_j[n] = y_j(t)\big|_{t=\left[\frac{T_p}{2}+nT_p\right]}, \;\; 0 \leq n \leq L-1. \tag{8}$$

The element $\mathbf{y}_j[n]$ is the row vector representing what we receive at n-th discrete slot on each of L available photodiodes.

Concerning the propagation scenarios, as described in the previous section, we distinguish that in the *LOS* case, the channel matrix can be represented by scalar coefficients h_{ij}, due to a very small channel length modeling the link connectivity among very close transmitting LEDs and receiving photodiodes. This reflects on good values –*i.e.*, low attenuation– of coefficients and severe path diversity loss. For the *ND-LOS* case, the reduced current at the photodiode means that the components of $\mathbf{Y}$ are smaller: this reflects on higher importance of the noise term since the $\mathbf{X}$ components are more attenuated. Lastly, the *NLOS* scenario models the partial / total absence of alignment between LEDs and photodiodes [24], and this may cause pulse overlapping if the PPM transmission rate is higher than the reciprocal of channel delay spread.

In regard to channel features, notice that different propagation scenarios imply different received signal properties. We make a special distinction between path diversity and spatially singular channels. When a *LOS* channel is considered, it is possible to have high spatial correlation so giving rise to only coding gain and no diversity gain. This does not mean to have singular channel matrices. On the other hand in the *NLOS* scenario the statistical uncorrelation among paths is highly possible.

3.1 Space-Time PPM Block Coding with rate issues

The matrix $\mathbf{X}$ logically describes the presence of a pulse on the time axis and the space (due to the LEDs' deployment). By considering the signal period T_s, the time length of each column is $L \cdot T_s$. Thus, the maximum rate in Spatial Multiplexing is

$$\mathcal{R}_{SM} = \frac{1}{L \cdot T_s} \log_2(L^{n_T}), \tag{9}$$

which becomes $\mathcal{R}_{SM} = T_s^{-1}$ in the case of $n_T = 2$ and $L = 2$, while for a single LED link (*i.e.*, $n_T = 1$) the data rate is $\mathcal{R} = 0.5 \cdot T_s^{-1}$. Notice that an increase of L without reducing T_s decreases the value of $\mathcal{R}$, while an increase of the number of LEDs / photodiodes increases the rate. So, the achievement of high rate values is due to both the possibility of having several LEDs / photodiodes, that can be installed also in small rooms, and the LED ability to quickly operate the electrical-to-optical conversion, this latter related to the modulation bandwidth of LEDs.

The expression given in (9) does not take into account the estimation of the channel. Without explaining here the rational leading to estimate the channel, we can anticipate that the transmission is *frame-oriented* with a frame length of N slots. Each frame is comprised of a number of N_e slots

(with $N_e << N$), dedicated to channel estimation, while N_d slots (*i.e.*, $N_d = N - N_e$) are used for data transmission.

Notice that, starting from the value of T_s, we can argue that the need for a new channel estimation is due when the channel changes, and this happens after a time $T_{channel}$ [s]. This value can be of the order of seconds since it depends on two main aspects. The first one is represented by the changes of propagation environment due to modifications in the room (*e.g.*, people walking, tables and reflective objects close to transmitter or receiver), while the second aspect is the user mobility. For the latter aspect, a sensor able to measure the receiver movement can be taken into account so to proceed with channel estimation when something changes. A conservative way of setting the time to wait for a new estimation is essentially due to the speed of a (pedestrian) user; so half a second can be a reasonable value. The value of N is given by $N = \lfloor T_{channel}/LT_s \rfloor$.

The information-based transmission rate *i.e.*, the rate of the data transmission by considering that some symbols are used for channel estimation, can be written as

$$\mathcal{R}_{(N_d,N_e)} = \frac{N_d}{(N_d + N_e)L \cdot T_s} \log_2(L^{n_T}). \tag{10}$$

In the general case of n_T transmitting LEDs and L-PPM modulation, the maximum number of possible matrix codewords (when SMP is considered) is L^{n_T}, and the l-th matrix (with $l \leq L^{n_T} \in \mathbb{R}^+$) is given by

$$\mathbf{C}_l = \begin{bmatrix} c_{11}^{(l)} & c_{12}^{(l)} & \dots & c_{1j}^{(l)} & \cdots & c_{1n_T}^{(l)} \\ c_{21}^{(l)} & c_{22}^{(l)} & \dots & c_{2j}^{(l)} & \cdots & c_{2n_T}^{(l)} \\ \vdots & \vdots & \vdots & \vdots & \vdots & \vdots \\ c_{i1}^{(l)} & c_{i2}^{(l)} & \dots & c_{ij}^{(l)} & \cdots & c_{in_T}^{(l)} \\ \vdots & \vdots & \vdots & \vdots & \vdots & \vdots \\ c_{L1}^{(l)} & c_{L2}^{(l)} & \dots & c_{Lj}^{(l)} & \cdots & c_{Ln_T}^{(l)} \end{bmatrix}, \tag{11}$$

which, in a more compact form, can be expressed as

$$\mathbf{C}_l = \left[\mathbf{c}_1^{(l)} \; \mathbf{c}_2^{(l)} \; \cdots \; \mathbf{c}_j^{(l)} \; \cdots \; \mathbf{c}_{n_T}^{(l)} \right], \tag{12}$$

being $\mathbf{c}_j^{(l)}$ the $[L \times 1]$ column vector representing the signal emitted by the j-th LED (related to the l-th codeword), under the following two constraints:

$$\sum_{i=1}^{L} c_{ij}^{(l)} = 1, \qquad \text{and} \qquad c_{ij}^{(l)} \in \{0, 1\}, \tag{13}$$

thus meaning that each column vector must contain all zeros with the exception of a sole 1. The expression used for evaluating rate implicitly contains some performance parameters like L, n_T together with $N_d + N_e$ and T_s. Since SMP allows high bit rate without taking care of error probability, in order to accomplish the task of achieving a minimum required rate, and guarantee a (required) maximum bit error probability for an assigned transmitting power, we must tackle with the following problem [5]:

[5]To be solved *offline*, when the VLC system is provisioned and installed.

$$\text{find a STBC}, \tag{14a}$$

$$\text{s.t.} \sum_{i=1}^{L}\sum_{j=1}^{n_T} c_{ij}^{(l)} c_{ij}^{(m)} = 0, \;\; l \neq m, \;\; l, m \in \mathfrak{M}, \;\; |\mathfrak{M}| = M, \tag{14b}$$

$$M \geq 2^{\frac{\mathcal{R}^\star L T_s (N_d + N_e)}{N_d}}, \tag{14c}$$

$$\sum_{i=1}^{L} c_{ij}^{(l)} = 1, \;\; \text{and} \;\; c_{ij}^{(l)} \in \{0, 1\}, \tag{14d}$$

$$\text{Pr}\{e\} \leq \text{Pr}\{e\}^\star. \tag{14e}$$

The first constraint is related to the choice of proposing codewords retaining the property of being trace orthogonal (see [53] for a non-orthogonal modulation case), that is, having

$$\text{Tr}\{\mathbf{C}_j^T \mathbf{C}_i\} = \begin{cases} 0 & j \neq i \\ n_T & j = i \end{cases} \tag{15}$$

The number of codewords must be at least M – the minimum value (from (14c)) required to achieve the minimum rate $\mathcal{R}^\star$. Moreover, M is the cardinality of $\mathfrak{M}$ that is the set containing all possible codewords retaining the property of being trace orthogonal. The constraints in (14d) are the same as reported in (13), while the last constraint (14e) is related to the error probability, whose expression will be detailed in Subsection 3.3, once introduced the receiver structure in Subsection 3.2.

The above problem is not feasible for each value of $\mathcal{R}^\star$ and $\text{Pr}\{e\}^\star$ (and also optical transmission power). Moreover, without the constraint (14d), it is also possible to have multiple pairs (L, n_T) guaranteeing the minimum rate $\mathcal{R}^\star$, even if each pair can lead to different $\text{Pr}\{e\}$.

Remark - On illumination issue

Before providing a simple example, let us remark here that we do not consider illumination in the above problem. The additional constraint should be on the received power at photodiodes expressed in lux (or equivalently in Watts). In this context it seems that PPM, exhibiting low Peak to Average Power Ratio (PAPR), can induce flickering and/or dimming. In this, we must differentiate the light emitted by LEDs and the light perceived by human eye. By resorting to the second Bloch's law (see chapter 3 in reference [63]) stating that the human eye is unable to distinguish two light flashes as different if they are sufficiently close in time. With operating frequencies well exceeding 1KHz we can argue that the light received by the human eye will be perceived as continuous. Moreover, since we deal with MIMO-PPM, there is always one LED in an ON state, so this solves the illumination issue.

A quick and simple example is that obtained by assuming a $(L = 2)$-PPM, performed over $(n_T = 2)$ LEDs; the matrix dimension is then $[2 \times 2]$. The maximum allowed number of matrix is L^{n_T} and the codewords are listed below

$$\mathbf{C}_1 = \begin{bmatrix} 1 & 0 \\ 0 & 1 \end{bmatrix}, \mathbf{C}_2 = \begin{bmatrix} 0 & 1 \\ 1 & 0 \end{bmatrix},$$

$$\mathbf{C}_3 = \begin{bmatrix} 1 & 1 \\ 0 & 0 \end{bmatrix}, \mathbf{C}_4 = \begin{bmatrix} 0 & 0 \\ 1 & 1 \end{bmatrix}. \tag{16}$$

By using all the matrices it is possible to achieve SMP while selecting only matrices $\mathbf{C}_3$ and $\mathbf{C}_4$, and also it is possible to achieve an orthogonal space-time block coding (in fact we have $\mathbf{C}_3^T\mathbf{C}_4 = \mathbf{0}_{2\times 2}$). Having Orthogonal STBC (OSTBC) means having TO-STBC. Using $\mathbf{C}_1$ and $\mathbf{C}_2$ allows having TO even if it does not guarantee OSTBC. This leads to use only 2 codewords, while the simultaneous use of 4 codewords allows achieving twice the data rate.

3.2 Receiver Architecture

Before introducing the receiver architecture, we analyze the properties retained by the space-time block codewords. As stated in the constraint (14.a), the codewords are trace-orthogonal. Usually this property is not guaranteed at the receiver since the rows and columns of the transmitted codewords are mixed by the channel. As a consequence, the channel knowledge at the receiver is fundamental to perform a correct detection/decoding process.

It is reasonable to assume that some pilot pulses can be transmitted, allowing the receiver to acquire sufficient information about the propagation environment. The receiver is comprised of

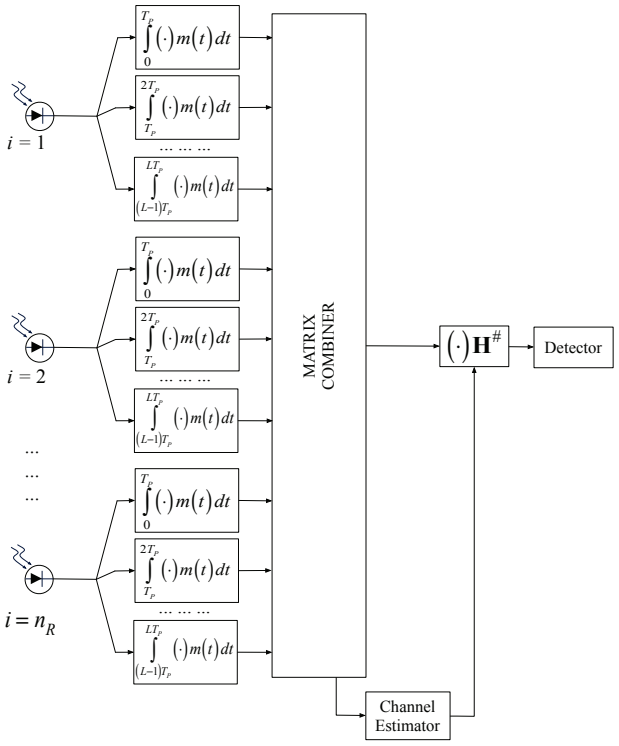

Figure 2: Block scheme of the receiver architecture. The i inputs are the signals received by n_R photodiodes, with $i = \{1, 2, \cdots, n_R\}$, each one filtered by an integrator bank. The matrix combiner collects all the filter outputs representing the estimated channel paths. The matrix (pseudo)-inversion operation is adopted for data detection.

two different logical operations that are (*i*) the *channel estimation*, and (*ii*) the *data detection*, as depicted in Figure 2.

Channel estimation

The *channel estimation* task requires special training sequences. By considering the channel representation in (6), it appears evident that for a matrix $\mathbf{C}$ equal to identity (*i.e.*, when $L = n_T$), the received matrix $\mathbf{Y}$ equates $(\mathbf{H}+\mathbf{W})$, thus meaning that in the estimation procedure the only source of error is noise. This implicitly means that a number of L symbols (with L equals to n_T) is needed for the estimation procedure.

Let us observe the receiver architecture depicted in Figure 2. At the i-th photodiode, the i-th signal is filtered by an integrator bank, in order to compare it with $m(t)$ that is the receiver mask (in this case, set equal to $x(t)$, so as to implement the matched filter). Moreover, each integrator is time-shifted, so that it can capture the energy on different L-PPM symbols/intervals; this is operated by each branch corresponding to each photodiode.

The matrix combiner collects all the filter outputs that represent the estimated channel paths. This simple estimation requires only $n_T \cdot T_s$ seconds,[6] under the simplifying assumption of a flat (frequency) channel, which is reasonable in very short range applications. Otherwise, mechanisms such as presented in reference [59] can reduce the delay spread, confirming the importance of channel estimation. This kind of estimation can be also improved via the transmission of more extensive pilot symbols (corresponding to N_e), so as to gather more energy. One important issue is related to how frequently pilot symbols are required to be sent in order to acquire channel information. The pilot rate, that is the rate used for sending pilots, depends on channel coherence time. We can argue that changes incur over a time horizon of seconds since the channel changes due to (*i*) movements performed by the receiver (user) or (*ii*) reflecting objects in the room. So setting pilot rate of the order of half a second should be sufficient to have sufficiently fresh estimates. ■

Data detection

In the more general case of signal spread by the channel, the performance of the estimator is strongly affected by synchronization. Under the quite satisfied assumption of minimum phase channel [59], we are required to have synchronization and a sufficient guard time in order to avoid pulse overlap and also a good estimation of the main path. Minimum phase channels are characterized to have main paths in the first samples. In order to avoid temporal ISI, it suffices to introduce guard times. However, if the channel is not minimum phase and presents long delays and main components in the middle of channel impulse response, the guard times are not suitable, and other mechanisms (*e.g.*, cyclic prefix), should be used.

As stated before, the presence of the channel mixes the spatial components, and even in the absence of noise, the trace properties of the matrices are altered due to channel. This suggests to spatially *solve* the channel by inverting it via a matrix inversion operation (in the case of squared matrix), or via the use of a pseudo-inverse matrix (used for rectangular matrix), as shown in Figure 2. From a computational point of view, this operation is inexpensive because it can be implemented through a shift register storing data and a simple algorithm (e.g., QR or Singular Value Decomposition) to operate the pseudo-inversion before a matrix product.

After the optical-to-electrical conversion operated by the photodiode, the received matrix $\mathbf{Y}$ should be processed in order to obtain a decision variable (*i.e.*, $\mathbf{Z}$) defined as follows

[6]This expression is due to the single receiver, which receives $Y = H$, in low noise condition. Thus, the channel is obtained by the output of each photodiode.

$$\mathbf{Z} = \mathbf{Y}\mathbf{H}^{\sharp} = \mathbf{X} + \mathbf{W}\mathbf{H}^{\sharp}, \tag{17}$$

where the symbol $^{\sharp}$ means (*i*) inversion or (*ii*) pseudo-inversion operation, depending on the matrix dimension *i.e.*, (*i*) squared or (*ii*) rectangular, respectively. This is a spatial Zero Forcing procedure (ZF).

Once obtained the decision variable $\mathbf{Z}$, the decided codeword will be

$$\hat{\mathbf{C}} = \arg\max_{i} \mathrm{Tr}\{\mathbf{C}_i^T \mathbf{Z}\}. \tag{18}$$

This decision mechanism directly comes from reference 17. When the space-filtered noise $\mathbf{W}\mathbf{H}^{\sharp}$ in (17) is negligible, $\mathbf{Z}$ approaches $\mathbf{X}$, and since the matrices are trace orthogonal we can recognize the transmitted codeword. Finally, the detection mechanism is applied to N_d consecutive matrix codewords. Notice that the following three steps: *i)* matrix inversion, *ii)* the product of the received matrix by the pseudo-inverse, and *iii)* data detection are quite simple to implement and not costly from a computational standpoint since L and n_T, n_R are limited to be in the range $[2, 16]$ for L, and $[1, 16]$ for n_T and/or n_R.

One important aspect is related to possible rank deficient property of the channel matrix. It is worthwhile noting that the channel estimation is affected by noise. So, even though the matrix rank is deficient (due to correlation among channels), the effect of noise affects the spatial correlation that is lost. This means we have a performance loss due to imperfect channel estimation, even if pseudoinversion can be still performed.

3.3 Performance evaluation

Starting from the orthogonality exhibited in the trace sense, it is possible to evaluate the performance in terms of bit error probability that leads to solve possible ambiguities in determining the n_T and M values needed for meeting constraints. The bit error probability $\Pr\{e\}$ can be upper-bounded by the so called Union-Bound as follows[7]:

$$\Pr\{e\} \leq \int_{\mathbf{H}} \sum_{i=1}^{M} \sum_{j=1, j\neq i}^{M} \Pr\{\hat{\mathbf{X}} = \mathbf{C}_j | \mathbf{C}_i, \mathbf{H}\} \Pr\{\mathbf{H}\}. \tag{19}$$

The role played by the channel is conditioning. It is reasonable that different statistical modeling *LOS*, *ND-LOS*, and *NLOS* lead to different $\Pr\{e\}$. Moreover, the inequality holds for the conditioned probability, and since the average on channel statistics is performed at right and left side (with the same weight that is channel probability density function) this holds also the unconditioned error probability. The upper bound for the term $\Pr\{\hat{\mathbf{X}} = \mathbf{C}_j | \mathbf{C}_i, \mathbf{H}\}$ can be evaluated starting from the detection criterion in (18), so the transmitted codeword $\mathbf{C}_i$ is –wrongly– decoded as $\mathbf{C}_j$ with the following pairwise upper bound on probability:

$$\Pr\{\hat{\mathbf{X}} = \mathbf{C}_j | \mathbf{C}_i, \mathbf{H}\} \leq \Pr\{\mathrm{Tr}\{\mathbf{C}_j^T \mathbf{Z}\} > \mathrm{Tr}\{\mathbf{C}_i^T \mathbf{Z}\}\}, \tag{20}$$

[7]We indicate with $\hat{\mathbf{X}}$ the detected codeword according to (18). So, we implicitly state that $\hat{\mathbf{X}} \equiv \hat{\mathbf{C}}$ even if, for sake of readability, we prefer here, to use the symbolic representation of the detected codeword $\hat{\mathbf{X}}$ related to the transmitted codeword $\mathbf{X}$.

that can be rewritten as:

$$\begin{gathered}\Pr\{\hat{\mathbf{X}}=\mathbf{C}_j|\mathbf{C}_i,\mathbf{H}\}\leq\\ \Pr\{\mathrm{Tr}\{\mathbf{C}_j^T\mathbf{C}_i+\mathbf{C}_j^T\mathbf{W}\mathbf{H}^\sharp\}>\mathrm{Tr}\{\mathbf{C}_i^T\mathbf{C}_i+\mathbf{C}_i^T\mathbf{W}\mathbf{H}^\sharp\}\},\end{gathered}\tag{21}$$

where we replaced $\mathbf{Z}=\mathbf{C}_i+\mathbf{W}\mathbf{H}^\sharp$.

Once noted that $\mathrm{Tr}\{\mathbf{A}+\mathbf{B}\}=\mathrm{Tr}\{\mathbf{A}\}+\mathrm{Tr}\{\mathbf{B}\}$, $\mathrm{Tr}\{\mathbf{C}_j^T\mathbf{C}_i\}=0$, and $\mathrm{Tr}\{\mathbf{C}_i^T\mathbf{C}_i\}=n_T$, we can rewrite the probability in (21) as follows

$$\begin{gathered}\Pr\{\hat{\mathbf{X}}=\mathbf{C}_j|\mathbf{C}_i,\mathbf{H}\}\leq\\ \Pr\{\mathrm{Tr}\{\mathbf{C}_j^T\mathbf{W}\mathbf{H}^\sharp\}>n_T+\mathrm{Tr}\{\mathbf{C}_i^T\mathbf{W}\mathbf{H}^\sharp\}\}\}.\end{gathered}\tag{22}$$

This last can be evaluated by resorting to a multivariate Gaussian distribution. Even if the nature of noise is different (Gaussian and Poisson), under the hypothesis of several light sources / reflections, the central limit theorem allows assuming the white noise as Gaussian. Then, by considering the linear combination induced among the noise samples by $\mathbf{C}_j$, $\mathbf{C}_i$, and $\mathbf{H}^\sharp$ –still providing a Gaussian random variable–, and also starting from a spatially white correlation for $\mathbf{W}$, once vectorized it through the $vec(.)$ operator, the new linearly combined noise variable $\mathfrak{n}$ should be higher[8] than n_T, *i.e.*

$$\Pr\{\hat{\mathbf{X}}=\mathbf{C}_j|\mathbf{C}_i,\mathbf{H}\}\leq\Pr\{\mathfrak{n}>n_T\}.\tag{23}$$

The Union Bound cannot be expressed in closed form since it depends on channel statistics. As anticipated, this implicitly suggests that the problem described in (14) should be tackled off-line during system planning and setup. Once the channel statistics are known (and this depends on several parameters and propagation scenarios), it is possible to determine the L, n_T and n_R combination for meeting the constraints on $\mathcal{R}^\star$, and $\Pr\{e\}^\star$. There is no algorithm to solve this but it should be simply computed for exhaustive search. This may appear costly, however since we are working with small numbers $L=2,4,8,16$, and the maximum rate is upper-bounded by SMP, giving indication of the feasibility of the system, we can conclude that this can be implemented with MATLAB calculus tools in few seconds. Other approaches as binary programming can be pursued to speed up the solution searching. As a conclusive remark about computational costs, we can argue that this is an off-line project tool for TO-SBTC, thus time saving is not an issue.

4 Numerical Results

The simulations have been developed under the parameter assumptions collected in Table 1 if not differently specified, both under the optimistic assumption of *perfect* channel knowledge at the receiver, and *imperfect* channel state information (at the receiver) due to estimation errors. The BER simulations are obtained via Monte-Carlo method. The channel model between each LED and photodiode has been obtained through the CandLES simulator [61]. In the simulations we

[8] As an example, let us consider the code represented by matrices $\mathbf{C}_3$ and $\mathbf{C}_4$, then (23) becomes

$$\begin{aligned}&\Pr\{\hat{\mathbf{X}}=\mathbf{C}_4|\mathbf{C}_3,\mathbf{H}\}=\\ &=\Pr\{(w_{21}-w_{11})(h_{11}^\sharp+h_{12}^\sharp)-(w_{22}-w_{12})(h_{21}^\sharp+h_{22}^\sharp)>n_T\}.\end{aligned}$$

assumed that the PPM time shift Δ equates $T_s = 12.98 \cdot 10^{-9}$ s. Also, the numerical results are averaged over the spatial area described by the assumptions reported in Table 1.

In the simulations, the SNR is referred both to optical and thermal noise in order to evaluate a worst case scenario. In particular, the overall noise is given by

$$\mathcal{N} = 2q(I_p + I_d)\Delta f + 4k_p T F \Delta f / R_f, \tag{24}$$

where I_p [A] is the average current, I_d [A] the dark current, Δf [Hz] the detector bandwidth, q electron charge, k_p [JK^{-1}] Boltzmann constant, T [K] the temperature, F noise factor, and R_f [Ω] amplifier feedback resistance. From (24), it follows that

$$SNR = \frac{(RP_r^{(opt)})^2}{2q(I_p + I_d)\Delta f + 4k_p T F \Delta f / R_f}, \tag{25}$$

that represents a worst case since optical and thermal noise components are simultaneously considered. Here R is the photodiode responsivity and $P_r^{(opt)}$ is the received optical power.

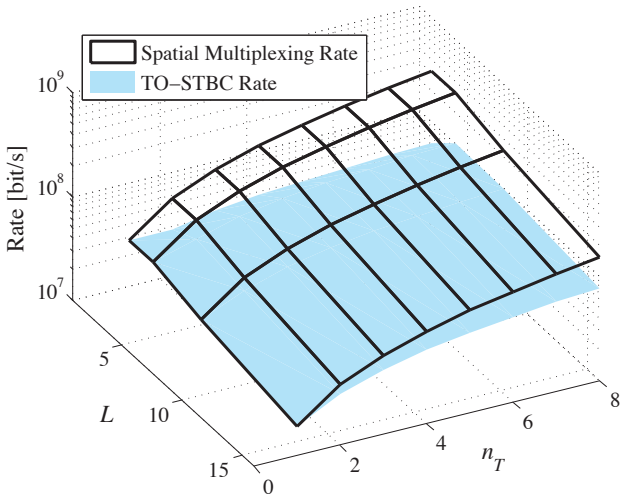

Figure 3: Achievable rates for different values of L and n_T, when SM and STBC are considered.

Figure 4 depicts the BER obtained for different values of L, and n_T, n_R in a *NLOS* scenario. Notice how while passing from $(L = n_T = n_R = 2)$ (with a rate of 38 Mbit/s) to $(L = 4, n_T = n_R = 2)$ (same rate), the BER decreases with the same slope since only a *coding gain*, in SNR sense, is obtained. The gain offered by the $(L = n_T = n_R = 4)$ configuration, with a rate of 156 Mbit/s, quickly achieves 10^{-9} at an SNR less than 14 dB, even if this configuration requires 2 more LEDs and 2 more photodiodes, w.r.t. the previous two configurations. The above gain can be observed also in terms of diversity. In fact the slope of $n_T = 4, n_R = 4$ and $L = 4$ case is higher since we are increasing the dimension of the MIMO system so leading to higher diversity gain). All the above results are obtained in line with the problem in (14) by asking for matrices to be TO.

The tri-dimensional plot in Figure 3 shows the simultaneous effect on achievable rate of the number L of PPM symbols and of the number n_T of LEDs, according to (9). The two surfaces are related to the SMP scenario, that is an upper bound for rate, and the transmission rate obtained by using TO-STBC. ¿From a feasibility point of view, the TO-STBC rate indicates the maximum

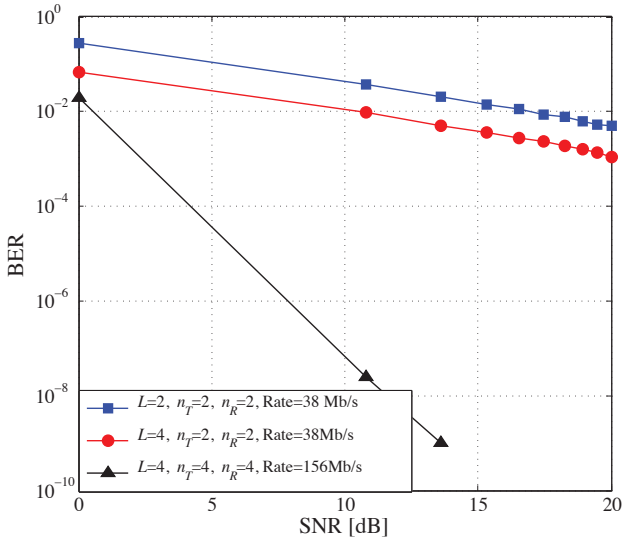

Figure 4: BER vs. SNR for MIMO-PPM with different values of L, n_T and n_R in NLOS scenario.

achievable transmission rate under the constraint on the codewords to maintain the TO property. This implicitly means that a rate over-bounding the STBC rate, for an assigned value of L and n_T, cannot retain the TO properties so its BER is higher with respect to the one obtained with TO.

By increasing L from 2 to 16, the value of $\mathcal{R}$ related to SMP decreases from 38.5 Mbit/s to 19 Mbit/s, when only 1 LED-photodiode pair is considered, while for 8 LED-photodiode pairs, the achievable rate falls from 308 Mbit/s to 154.5 Mbit/s (with *blue* filter). This suggests that increasing the order of L-PPM modulation is not worth, while increasing the number of LEDs / photodiodes allows achieving very high rates. The limitation given by the L-PPM order may be fixed by adapting the T_s value to make the product $(L \cdot T_s)$ in (9) constant. In order to do so, a technological issue should be tackled since, as previously anticipated, this is strictly tied to the ability of LEDs to quickly perform the electrical-to-optical conversion. Regarding the STBC rate, its behavior with one LED is the same of SMP, while for $L = 16$ the maximum rate is around 150 Mbit/s.

Furthermore, due to the important role of channel knowledge, we evaluated the channel robustness, as compared to an *imperfect* channel knowledge for statistically modeled channels. Even if the channel is slowly time-variant, when the relative positions between LEDs and photodiodes change, and new reflections are present, the propagation scenario is different. So, a sporadic pilot signaling is needed via pilots for channel knowledge acquisition. Under the hypothesis of having a data link layer able to operate error detection, the new estimation may be performed once an error has been detected. Alternatively, this can also be operated in real devices via accelerometer sensors, able to detect receiver movements.

In Fig. 5, increasing values of σ_h^2 refers to a imperfect channel state information detection; in practical scenarios, this may be due to users moving in the room (*i.e.*, interferers), photodiode moved or external light sources added to the LED signal at the photodiode (*i.e.*, ambient noise).

The channel model is obtained through the use of CandLES simulator, and the comparison with Maximum Likelihood (ML) and Minimum Mean Square Error (MMSE) has been reported. We

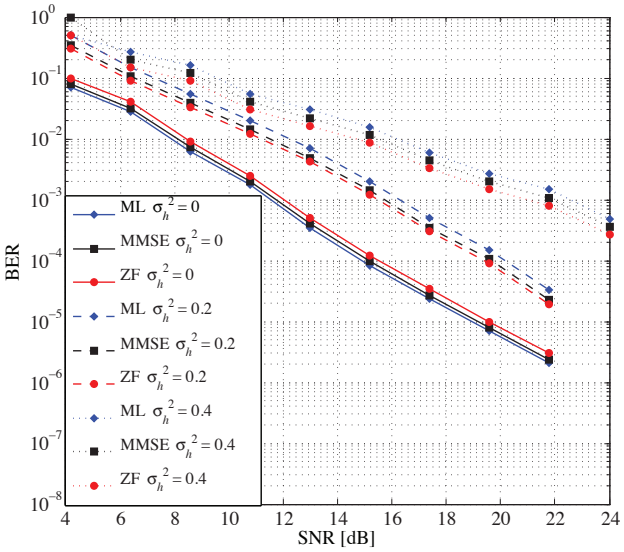

Figure 5: BER vs. SNR for MIMO-PPM with different level of estimation errors, in the case of $[2 \times 2]$ system with 2-PPM.

considered the term σ_h^2 related to the amplitude of channel $h(t)$, formally defined as

$$\sigma_h^2 = 1 - \frac{\int_T |\hat{h}(t)|^2 dt}{\int_T |h(t)|^2 dt}, \tag{26}$$

being $\hat{h}(t)$ the estimation of the channel.

Under the assumption that the channel is perfectly known at the receiver, the performance in terms of BER are the same and the curves are very closed to the following ranking: ML better than MMSE, and MMSE better than ZF. When the knowledge is corrupted by errors *i.e.*, $\sigma_h^2 = 0.2$, the BER increases, and also the performance hierarchy changes. ZF operated on $\mathbf{Z}$ is better than MMSE and ML, because ZF results to be less sensible to channel estimation errors, thanks to trace operator w.r.t. the effect induced on the other approaches. The same behavior is experienced when $\sigma_h^2 = 0.4$, even if the BER values are higher (around 10^{-3} at $SNR = 18$ dB), while the perfect channel knowledge assures BER values below 10^{-6}, for the same SNR.

In order to validate the proposed technique w.r.t. other existing contributions, we provide a performance comparison, and considered the schemes proposed by Ntogari *et al.* in [42], Popoola *et al.* in [43], Abou-Rjeily in [44] since they represent recent works that are the best candidates for comparison purpose. The results are obtained assuming:

1. 4 LEDs and 1 photodiode with 4-PPM, for the solution in [43] since in this shape that scheme has been developed,
2. 2 LEDs and 2 photodiode, for the Alamouti code presented in [42] since the Alamouti-like scheme has been proposed for 2×1 and 2×2 systems,
3. 4 LEDs and 1 photodiode with a 4-PPM, for the one proposed by Abou-Rjeily in [44],
4. 4 LEDs and 1 photodiode with 4-PPM, and 2 LEDs and 2, 2-PPM of the proposed TO-STBC for a fair comparison.

The simulation scenario is the same as depicted in [43], *i.e.*, the position of the user is evaluated (*i*) "under" and (*ii*) "far away" the LED, corresponding respectively to the *room center*, and the *room corner*. We have tested the various techniques in two different propagation scenarios, respectively under the assumptions of *perfect* ($\sigma_h^2 = 0$) and *imperfect* ($\sigma_h^2 = 0.15$) channel knowledge. For comparison purpose, we assumed for the three techniques common room configuration parameters, as shown in Table 1.

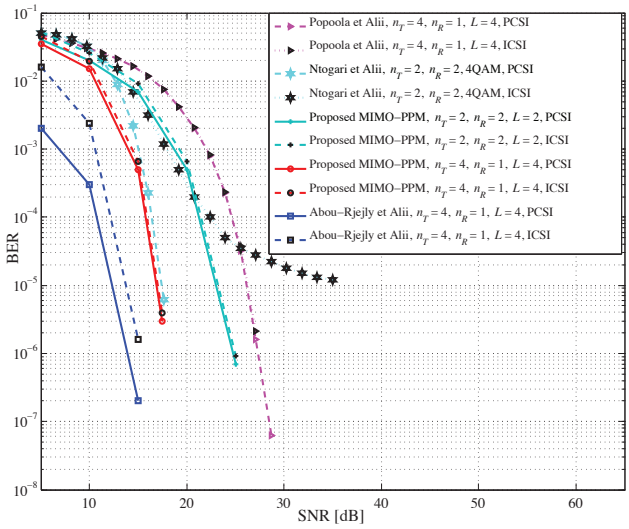

Figure 6: BER vs. SNR for different approaches, in room center scenario. The proposed scheme MIMO-PPM is compared to the works by Ntogari *et al.* [42], Popoola *et al.* [43] and Abou-Rjeily *et al.* in [44].

Consider Figure 6 and the behavior of the receiver in the *center* of the room. The Abou-Rjeily *et alii* approach outperforms the others because at low SNR it achieves very low BER.
In the case of Imperfect Channel State Information (ICSI) the performance is, as expected, not as satisfactory. For both the n_T, n_R, L configurations described before, our proposed scheme is able to perform better w.r.t. the ones of Popoola's and Ntogari's one, while it fails w.r.t. [44]. The gap is 5 dB. Not surprisingly, all the systems compared here under the ICSI case show worse performance compared to Perfect Channel State Information (PCSI). A particular note should be given for the Ntogari's (Alamouti-like) scheme that presents an error floor when ICSI is considered.

A different behavior occurs when the receiver is far from the LEDs (*i.e.*, in the room *center*) as reported in Fig.7. The SNR values achieving low BERs are higher w.r.t. the previous case. Also in this case, the scheme proposed in reference [44] has the best performance; our TO-STBC differs by approximatively 5 dB. On the other hand, the TO-STBC performs better w.r.t. the schemes proposed in [42] by Ntogari *et al.*, and Poopola *et al.*

When performance is evaluated in the corner position with ICSI, BER increases in all schemes.

The above comparison is perhaps not entirely fair because each system uses different assumptions about achievable transmission rates. In the performed simulations, all the considered systems are compared under the assumption of the same pulse duration, and the same power transmission level. An interesting way of showing the possibilities offered by the above cited systems is reported in Figure 8, where for a BER of 10^{-5}, the SNR needed and the transmission rate $\mathcal{R}$ are reported and compared to the Shannon capacity curves for the simple case $n_T = n_R = 1$. Note that the

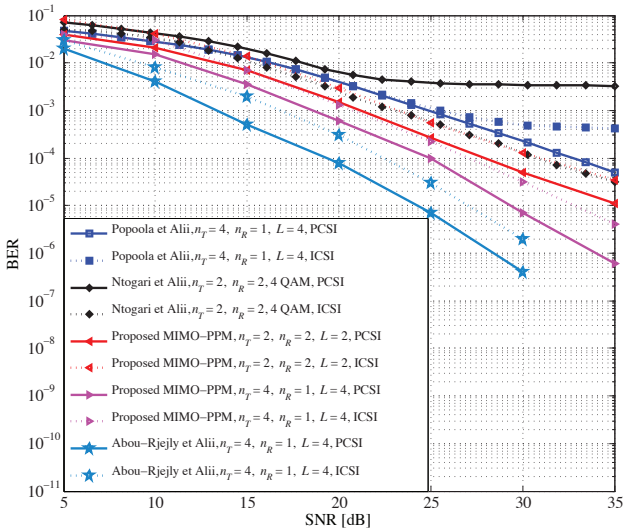

Figure 7: BER vs. SNR for different approaches, in room corner scenario. The proposed scheme MIMO-PPM is compared to the works by Ntogari *et al.* [42], Popoola *et al.* [43] and Abou-Rjeily *et al.* in [44].

Shannon curve does not consider the features typical of the optical link (no negative signals and Gaussian and Poisson disturbance), so in this sense it is a bit optimistic since, due to a bias optical signal, the power to be spent must be higher so it is an upper bound.

Safari *et al.* [49] is able to achieve the target BER with a very low SNR; however, at the expense of reducing transmission rate of the PAM-based modulation due to the repetition coding used (N in the plot indicates the number of repetitions of the same symbol). On the other hand, the target BER the scheme proposed by Poopola *et al.* [43] achieves a very good transmission rate (*i.e.*, 77 Mbit/s), at the expense of transmission power. This is not a heavy drawback if we resort to a downlink scheme, although it strongly increases the negative effect if an uplink is considered. A modestly higher performance, expressed in terms of rate, is achieved by Ntogari *et al.* [42] under the assumption of 4-QAM even if it requires perfect channel knowledge and high transmission power. They achieve 150 Mbit/s. The MIMO-OOK (independent OOK transmission of 4 different LEDs as SM) performs well in terms of rate (300 Mbit/s), while fails on power efficiency. SISO-OOK is under MIMO-OOK in terms of rate even if it requires less power to achieve the target BER. SISO 4-PPM is a bit worse w.r.t. SISO OOK due to the spectral inefficiency of PPM while it gains in terms of SNR.

Regarding the contribution in reference [44] that exhibits the best considered BER, it clearly is in the left part of the plot because low SNR is required for the target BER. Since that scheme presents matrices of dimensions $Ln_T \times n_T$, this reduces its rate because $Ln_T T_s$ are needed to transmit a codeword. Finally, the proposed TO-STBC performs well for the $n_T = 4, n_R = 1$, 4-PPM because it is at the same level of MIMO-OOK with a considerable gain in terms of power. It has half of the rate of Ntogari's approach but with less power, more robustness w.r.t. channel knowledge, and has simplicity of realization. The $n_T = 2, n_R = 2$, 2-PPM scheme is in-between w.r.t. $n_T = 4$, $n_R = 1$, 4-PPM performances of the proposed scheme, and the one of reference [48].

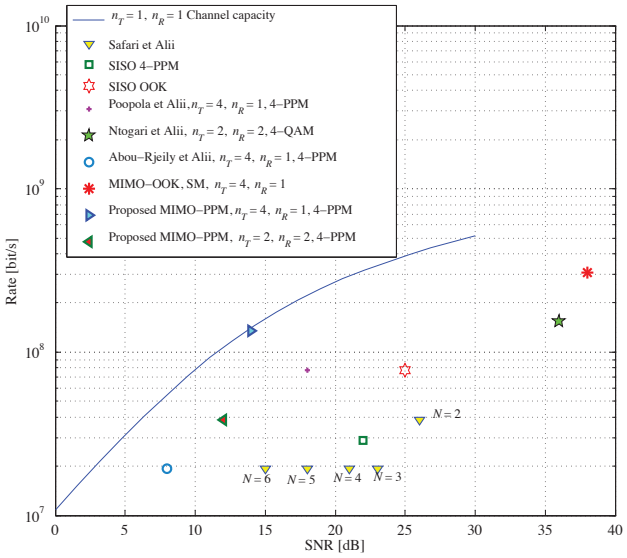

Figure 8: Rate vs. SNR at BER 10^{-5} for different schemes with respect to traditional SISO channel Shannon capacity.

5 Conclusions

In this paper we have presented a MIMO-PPM scheme based on STBC under the constraint of matrices to be trace orthogonal (TO-STBC). The proposed technique aims to enhance performance in indoor VLC system. The TO-STBC architecture aims at finding the so called *via media* between a low BER and a high data rate without requiring complex hardware implementation. Even if PPM is known to be bandwidth inefficient, through the use of multiple LEDs and photodetectors it is possible to gain in rate and BER, and counterbalance any PPM inefficiencies.

The performance offered by this system is comparable with contemporary schemes proposed in the literature. In detail, the proposed scheme does not present the lowest BER or the highest rate but it stresses the transmission rate–error-rate trade-off. Specifically, we argue that the compromise between these performance metrics is superior to what exists in the current literature. Very low BER-achieving systems lose more than the proposed approach in terms of rate, while better systems in terms of rate are required to use more transmission power to achieve similar performance.

References

[1] D. C. O'Brien et al., "Indoor Visible Light Communications: challenges and prospects," *Proc of SPIE*, vol. 7091, 2008.

[2] M. Kavehrad, "Sustainable energy-efficient wireless applications using light," *IEEE Communications Magazine*, December 2010.

[3] T. Borogovac, M. Rahaim, and J. B. Carruhers, "Spotlighting for visible light communications and illumination," in *Workshop on Optical Communications, GLOBECOM*, 2010.

[4] F. Szczot, "Safety problems in free space optical transmission," *Proceedings of SPIE*, vol. 6159, 2006.

[5] J. Vucic et al., "513 Mbit/s Visible Light Communications Link Based on DMT-Modulation of a White LED," *Journal of Lightwave Technology*, vol. 28, no. 24, 2010.

[6] J. Vucic, C. Kottke, K. Habel, and K.-D. Langer, "803 Mbit/s Visible Light WDM Link based on DMT Modulation of a Single RGB LED Luminary," in *Optical Fiber Communication Conference and Exposition (OFC/NFOEC) and the National Fiber Optic Engineers Conference*, March 2011.

[7] J. Armstrong and B. Schmidt, "Comparison of asymmetrically clipped optical ofdm and dc-biased optical ofdm in awgn," *Communications Letters, IEEE*, vol. 12, no. 5, pp. 343–345, 2008.

[8] L. Chen, B. Krongold, and J. Evans, "Performance analysis for optical ofdm transmission in short-range im/dd systems," *Lightwave Technology, Journal of*, vol. 30, no. 7, pp. 974–983, 2012.

[9] Y. F. Liu, C. H. Yeh, C. W. Chow, Y. Liu, Y. L. Liu, and H. K. Tsang, "Demonstration of bi-directional led visible light communication using tdd traffic with mitigation of reflection interference," *Opt. Express*, vol. 20, no. 21, pp. 23 019–23 024, Oct 2012. [Online]. Available: http://www.opticsexpress.org/abstract.cfm?URI=oe-20-21-23019

[10] J. Dang and Z. Zhang, "Comparison of optical ofdm-idma and optical ofdma for uplink visible light communications," in *Wireless Communications Signal Processing (WCSP), 2012 International Conference on*, 2012, pp. 1–6.

[11] M. Biagi, A. Vegni, and T. Little, "LAT Indoor MIMO-VLC –Localize, Access and Transmit–," in *Proc. of Intl. Workshop on Optical Wireless Communications*, Pisa, Italy, October 22 2012.

[12] O.-S. and Health-Branch-Labour-Department, *Simple Guide to Health Risk Assessment - Office Environment Series OE 2/99*, 1998.

[13] J. Grubor, S. Randel, K. Langer, and J. W. Walewski, "Broadband Information Broadcasting Using LED-Based Interior Lighting," *Journal of Lightwave Technology*, vol. 26, pp. 3883–3892, 2008.

[14] S. Hranilovic and F. Kschischang, "A Pixelated MIMO Wireless Optical Communication System," *IEEE Journal of Selected Topics in Quantum Electronics*, vol. 12, pp. 859–874, July/August 2006.

[15] D. Gesbert, M. Shafi, D. shan Shiu, P. Smith, and A. Naguib, "From Theory to Practice: An Overview of MIMO Space-Time Coded Wireless Systems," *IEEE J. Sel. Areas Commun.*, vol. 21, pp. 281–302, April 2003.

[16] P. Butala, H. Elgala, and T. Little, "SVD-VLC: a novel capacity maximizing VLC MIMO system architecture under illumination constraints," in *IEEE Globecom Workshops* , December 2013, pp. 1087–1092.

[17] ——, "Sample Indexed Spatial Orthogonal Frequency Division Multiplexing ," *Chinese Optics Letters (to appear)* , vol. 12, 2014.

[18] S. M. Hass, S. J. H., and V. Tarokh, "Space-time codes for wireless optical communications," *EURASIP Journal of Applied Signal Processing*, vol. 3, pp. 211–220, 2002.

[19] P. Haigh, Z. Ghassemlooy, F. Bausi, I. Papakonstantinou, H. Le Minh, S. Tedde, O. Hayden, and F. Cacialli, "Organic visible light communications: Recent progress," in *Transparent Optical Networks (ICTON), 2014 16th International Conference on*, July 2014, pp. 1–5.

[20] P. Haigh, Z. Ghassemlooy, I. Papakonstantinou, F. Tedde, S. Tedde, O. Hayden, and S. Rajbhandari, "A mimo-ann system for increasing data rates in organic visible light communications systems," in *Communications (ICC), 2013 IEEE International Conference on*, June 2013, pp. 5322–5327.

[21] P. Haigh, Z. Ghassemlooy, H. L. Minh, S. Rajbhandari, F. Arca, S. Tedde, O. Hayden, and I. Papakonstantinou, "Exploiting equalization techniques for improving data rates in organic optoelectronic devices for visible light communications," *Lightwave Technology, Journal of*, vol. 30, no. 19, pp. 3081–3088, Oct 2012.

[22] S. Jivkova, B. Hristov, and M. Kavehrad, "Power-efficient Multispot-diffuse Multiple-input-multiple-output Approach to broad-band Optical Wireless Communications," *IEEE Trans. Veh. Technol.*, vol. 53, no. 3, pp. 882–889, May 2004.

[23] L. Zeng, D. O'Brien, H. Minh, G. Faulkner, K. Lee, D. Jung, Y. Oh, and E. T. Won, "High data rate Multiple Input Multple Output (MIMO) Optical Wireless Communications using White LED Lighting," *IEEE J. Sel. Areas Commun.*, vol. 27, no. 9, pp. 1654–1662, December 2009.

[24] R. M. R. Mesleh, H. Helgala and H.Haas, "Performance of optical spatial modulation with transmitters-receivers alignment," *IEEE Communication Letters*, vol. 15, no. 1, pp. 79–81, 2011.

[25] T. Fath and H. Haas, "Performance Comparison of MIMO Techniques for Optical Wireless Communications in Indoor Environments," *IEEE Transactions on Communications*, vol. 61, pp. 733–742, February 2013.

[26] ——, "Optical Spatial Modulation using Colour LEDs," in *IEEE ICC 2013 - Optical Networks and Systems*, June 2013, pp. 3938–3942.

[27] M. Di Renzo, H. Haas, A. Ghrayeb, S. Sugiura, and L. Hanzo, "Spatial modulation for generalized mimo: Challenges, opportunities, and implementation," *Proceedings of the IEEE*, vol. 102, no. 1, pp. 56–103, Jan 2014.

[28] J. Esch, "Prolog to "spatial modulation for generalized mimo: Challenges, opportunities, and implementation"," *Proceedings of the IEEE*, vol. 102, no. 1, pp. 53–55, Jan 2014.

[29] G. Yun and M. Kavehrad, "Spot-diffusing and Fly-Eye Receivers for Indoor Infrared Wireless Communications," in *Proc. of IEEE Int. Conf. Selected Topics in Wireless Communications*, 1992, pp. 262–265.

[30] S. Wilson, M. Brandt-Pearce, Q. Cao, and J. Leveque, "Optical MIMO transmission using Q-ary PPM for atmospheric channels," in *Proc. 37th Asilomar Conf. Signals, Systems and Computers*, vol. 19, Pacific Grove, CA, November 12 2003, p. 2361.

[31] M. Garfield, C. Liang, T. Kurzweg, and K. R. Dandekar, "MIMO space-time Coding for Diffuse Optical Communication," *Microw. Opt. Technol. Lett.*, vol. 48, pp. 1108–1110, June 2006.

[32] S. Hranilovic and F. R. Kschischang, "Short-range Wireless Optical Communication using Pixilated Transmitters and Imaging Receivers," in *Proc. 2004 IEEE Int. Conf. Communications*, Paris, France, June 20–24 2004.

[33] R. Mesleh, R. Mehmood, H. Elgala, and H. Haas, "Indoor MIMO Optical Wireless Communication using Spatial Modulation," in *Proc. IEEE Int. Conf. Communications (ICC)*, Cape Town, South Africa, May 23–27 2010, pp. 1–5.

[34] P. Butala, H. Elgala, and T. Little, "Performance of Optical Spatial Modulation and Spatial Multiplexing with Imaging Receiver," in *IEEE WCNC'14*, Istanbul, Turkey, April 2014.

[35] D. O'Brien, "Multi-input multi-output (MIMO) Indoor Optical Wireless Communications," in *Proc. of Signals, Systems and Computers, Conference Record of the Forty-Third Asilomar*, November 1-4, 2009, pp. 1636–1639.

[36] K.-H. Park, Y.-C. Ko, and M.-S. Alouini, "On the Power and Offset Allocation for Rate Adaptation of Spatial Multiplexing in Optical Wireless MIMO Channels," in *Proc. of 7th Intl. Wireless Communications and Mobile Computing Conference*, July 4-8 2011, pp. 141–146.

[37] A. Burton, H. L. Minh, Z. Ghassemlooy, E. Bentley, and C. Botella, "Experimental demonstration of 50-mb/s visible light communications using 4 , $times$, 4 mimo," *Photonics Technology Letters, IEEE*, vol. 26, no. 9, pp. 945–948, May 2014.

[38] F.-M. Wu, C.-T. Lin, C.-C. Wei, C.-W. Chen, H.-T. Huang, and C.-H. Ho, "1.1-gb/s white-led-based visible light communication employing carrier-less amplitude and phase modulation," *Photonics Technology Letters, IEEE*, vol. 24, no. 19, pp. 1730–1732, Oct 2012.

[39] A. Khalid, G. Cossu, R. Corsini, P. Choudhury, and E. Ciaramella, "1-gb/s transmission over a phosphorescent white led by using rate-adaptive discrete multitone modulation," *Photonics Journal, IEEE*, vol. 4, no. 5, pp. 1465–1473, Oct 2012.

[40] J.-h. Choi, E.-b. Cho, Z. Ghassemlooy, S. Kim, and C. Lee, "Visible light communications employing ppm and pwm formats for simultaneous data transmission and dimming," *Optical and Quantum Electronics*, pp. 1–14, 2014. [Online]. Available: http://dx.doi.org/10.1007/s11082-014-9932-0

[41] D. Tsonev, S. Sinanovic, and H. Haas, "Practical mimo capacity for indoor optical wireless communication with white leds," in *Vehicular Technology Conference (VTC Spring), 2013 IEEE 77th*, June 2013, pp. 1–5.

[42] G. Ntogari, T. Kamalakis, and T. Sphicopoulos, "Performance analysis of space time block coding techniques for indoor optical wireless systems," *Selected Areas in Communications, IEEE Journal on*, vol. 27, no. 9, pp. 1545 –1552, december 2009.

[43] W. Popoola, E. Poves, and H. Haas, "Spatial pulse position modulation for optical communications," *Lightwave Technology, Journal of*, vol. 30, no. 18, pp. 2948 –2954, sept.15, 2012.

[44] C. Abou-Rjeily and W. Fawaz, "Space-time codes for mimo ultra-wideband communications and mimo free-space optical communications with ppm," *Selected Areas in Communications, IEEE Journal on*, vol. 26, no. 6, pp. 938–947, 2008.

[45] C. Abou-Rjeily and M. Bkassiny, "Unipolar space-time codes with reduced decoding complexity for th-uwb with ppm," *Wireless Communications, IEEE Transactions on*, vol. 8, no. 10, pp. 5086–5095, 2009.

[46] C. Abou-Rjeily, "Orthogonal space-time block codes for binary pulse position modulation," *Communications, IEEE Transactions on*, vol. 57, no. 3, pp. 602–605, 2009.

[47] C. Abou-Rjeily and Z. Baba, "Achieving full transmit diversity for ppm constellations with any number of antennas via double position and symbol permutations," *Communications, IEEE Transactions on*, vol. 57, no. 11, pp. 3235–3238, 2009.

[48] V. Tarokh, N. Seshadri, and A. R. Calderbank, "Space-time codes for high data rate wireless communication: performance criterion and code construction," *IEEE Trans. Inf. Theor.*, vol. 44, no. 2, pp. 744–765, Sep. 2006. [Online]. Available: http://dx.doi.org/10.1109/18.661517

[49] M. Safari and M. Uysal, "Do we really need ostbcs for free-space optical communication with direct detection?" *Wireless Communications, IEEE Transactions on*, vol. 7, no. 11, pp. 4445–4448, 2008.

[50] X. Song and J. Cheng, "Subcarrier intensity modulated mimo optical communications in atmospheric turbulence," *Optical Communications and Networking, IEEE/OSA Journal of*, vol. 5, no. 9, pp. 1001–1009, Sept 2013.

[51] E. Bayaki and R. Schober, "On space-time coding for free-space optical systems," *Trans. Comm.*, vol. 58, no. 1, pp. 58–62, Jan. 2010. [Online]. Available: http://dx.doi.org/10.1109/TCOMM.2010.01.080142

[52] H. Haas, "Wireless data from every light bulb," in *TED - Ideas worth Spreading*, 2011, p. available at $http://www.ted.com/$.

[53] S. Barbarossa, "Trace-orthogonal design of mimo systems with simple scalar detectors, full diversity and (almost) full rate," in *Signal Processing Advances in Wireless Communications, 2004 IEEE 5th Workshop on*, 2004, pp. 308–312.

[54] J. M. Kahn and J. R. Barry, "Wireless infrared communications," *Proceedings of the IEEE*, vol. 85, no. 2, pp. 265–298, 1997.

[55] H. M. H. Shalaby, "Effect of thermal noise and apd noise on the performance of oppm-cdma receivers," *Lightwave Technology, Journal of*, vol. 18, no. 7, pp. 905–914, 2000.

[56] J. R. Barry, *Wireless Infrared Communications*. Kluwer, 1994.

[57] R. Ramirez-Iniguez, S. M. Idrus, and Z. Sun, *Optical Wireless Communications*. CRC Press, 2008.

[58] J. M. Kahn and J. R. Barry, "Wireless infrared communications," *Proceedings of the IEEE*, vol. 85, no. 2, pp. 265–298, February 1997.

[59] H. L. Minh et al., "100-Mb/s NRZ Visible Light Communications Using a Postequalized White LED," *IEEE Photonics Technology Letters*, vol. 21, no. 15, pp. 1063–1065, 2009.

[60] M. Biagi, T. Borogovac, and T. Little, "Adaptive receiver for indoor visible light communications," *Lightwave Technology, Journal of*, vol. 31, no. 23, pp. 3676–3686, Dec 2013.

[61] T. B. M. Rahaim and J. B. Carruthers, "Candles: Communications and lighting emulation software," in *Fifth ACM International Workshop on Wireless Network Testbeds, Experimental Evaluation and Characterization*, 2010.

[62] A.M.Vegni and M.Biagi, "An Indoor Localization Algorithm in a Small-Cell LED-based Lighting System," in *Proc. of IEEE Intern. Conf. on Indoor Positioning and Indoor Navigation*, 2012.

[63] A. K. Jain, *Fundamentals of Digital Image Processing*. Prentice Hall, 1989.